DESIGN AND PERFORMANCE OF A PROTOTYPE BOROHYDRIDE FUEL CELL AND CONTROL SYSTEM

BY

TAPAN C. PATEL

THESIS

Submitted in partial fulfillment of the requirements
for the degree of Master of Science in Mechanical Engineering
in the Graduate College of the
University of Illinois at Urbana-Champaign, 2012

Urbana, Illinois

Adviser:

Dr. George Miley

ABSTRACT

A direct borohydride fuel cell stack with a novel integrated manifold, along with a control system, was designed, manufactured and studied. Two fuel cell stacks were built and demonstrated. The main objective was to build these stacks to achieve a power level of 100 watts. The control system was designed to allow for fuel cell startup and to self-sustain the stack. One 12 cell stack was able to achieve 168 Watts at 14 W/cell or 140 mW/cm^2, with the second 9 cell stack only able to achieve 5.6 W/cell , 56 mW/cm^2, or 54 W. A design flaw was encountered which did not allow for extended operation of the stack. A quick "fix" solution to this problem was attempted in the second stack. The solution, however, introduced several new issues which resulted in degraded performance. Nevertheless, the control system showed the cell stack can operate independently. This study has provided valuable information about the cell stack and control system performance which will be extremely helpful in future designs.

ACKNOWLEDGEMENTS

This project would not have been possible without the support of many people. I would like to thank my advisor, Dr. George H. Miley, for providing me with the opportunity to work on such an interesting topic. Also, many thanks to Dr. Kyu-Jung Kim and Dr. Nie Luo whose expertise and recommendations were extremely valuable. I would also like to thank my family, especially my parents, for their support during my research, and my friends who endured this long process with me. I would like to acknowledge the U.S. Army Corps of Engineers ERDC-CERL research lab, and specifically my mentor Nick Josefik, where I also conducted fuel cell research over the duration of the degree. My experiences there were instrumental in the successful completion project. Finally, thanks to Lockheed Martin and NPL Associates Inc., who funded the project.

TABLE OF CONTENTS

CHAPTER 1: INTRODUCTION

This thesis is concerned with the design and performance of a direct borohydride fuel cell and control system which is aimed to provide a high energy, high power density alternative option to several existing fuel cell technologies.

The increasing demand for clean and efficient fuels has recently led to the widespread development of fuel cell technologies. Market volatility and the ever decreasing resources of oil-based fuels such as gasoline have further accelerated research in this area. Fuel cells are believed to have the potential to supply power for a wide range of applications from large buildings to portable laptops and cell phones. The current prohibitive cost of fuel cells has prevented widespread use, but stringent goals and increased research efforts across the world are aimed at decreasing this cost.

1.1 Overview of Fuel Cells

A fuel cell is an electrochemical device which produces electricity as long as a fuel and oxidizer are provided [1]. The basic operation of a fuel cell was discovered in 1839 by lawyer and scientist, William Grove. Today several types of fuel cells are under development, each design with its advantages and disadvantages. These fuel cells vary by operating temperature, fuels, catalyst selections, and other parameters. The most common type of cell is the hydrogen – oxygen fuel cell which is seen as a promising solution to replace gasoline as the fuel for automobiles.

This type of fuel cell employs a Proton Exchange Membrane (PEM) and hydrogen as the fuel with oxygen as the oxidizer. Although this type of fuel cell is relatively simplistic in its

operation, compared to other fuels, there are significant disadvantages with the storage of hydrogen. Hydrogen has the highest energy density of any known fuel, but in ambient conditions it is a gas and needs to be stored under high pressure to achieve any practical volumetric energy density. However, the compression process is energy intensive and requires costly equipment.

Due to the storage limitations, liquid fuels whose chemical structure is composed of hydrogen are being sought as alternatives to the pure gas form. For example, methanol (CH_3OH) and sodium borohydride ($NaBH_4$) are both being considered as viable alternatives. The advantage of these fuels is that they are stored in a liquid form, which significantly reduces the logistical burden associated with their storage and transport. Furthermore, both provide high energy densities.

Recent research has shown that direct borohydride/air fuel cells provide higher open circuit voltages than both hydrogen/oxygen and methanol/air fuel cells [2]. With the high theoretical energy density of sodium borohydride (9.3 Wh/g), this type of fuel cell is promising. Sodium borohydride is usually found in a solid form and results in a highly exothermic and unstable reaction in water. However, sodium borohydride is highly soluble in aqueous sodium hydroxide solutions of approximately 10 to 15% (which act as a stabilizer) and can therefore be stored in a liquid form, which is advantageous due to ease of storage and transport. Another benefit of this fuel is that the byproduct of the fuel cell reaction is sodium metaborate ($NaBO_2$) which is environmentally friendly and can be potentially recycled into sodium borohydride [3].

There is significant motivation to use hydrogen peroxide (H_2O_2) as the oxidizer instead of air at the cathode. It is widely known that the oxygen reduction process on the cathode is 6 orders of magnitude lower than that of the hydrogen oxidation process at the anode [4].

Therefore, the limiting kinetics of the cathode affects overall fuel cell performance. The oxygen reduction reaction is as follows:

$$O_2 + 4H^+ + 4e^- \rightarrow 2H_2O \quad (1)$$

The hydrogen peroxide reduction reaction is as follows:

$$H_2O_2 + 2H^+ + 2e^- \rightarrow 2H_2O \quad (2)$$

As seen, the oxygen reduction requires the transfer of 4 electrons and therefore has a reduced probability of occurrence, due to the higher activation over potential, when compared to the peroxide reduction which requires the transfer of two electrons. Thus, utilizing hydrogen peroxide at the cathode will yield improved cell performance characteristics.

There are additional benefits for using hydrogen peroxide as an oxidant. Firstly, in applications where oxygen/air is not freely available, such as in underwater vehicles, this combination provides an effective alternative. Secondly, hydrogen peroxide is environmentally friendly and is in a liquid form which makes it easier to handle. Although there are some safety considerations due to its high oxidation potential, its handling is nevertheless simpler than that of gases. Additionally, its wide use in the chemical industry has led to high production volumes and low cost.

This thesis will discuss the design and performance characteristics of a direct borohydride fuel cell (DBFC) which utilizes sodium borohydride as a fuel and hydrogen peroxide as the oxidizer. It will also discuss the design of a prototype control system for this application.

1.2 Background of Direct Borohydride Fuel Cells

The construction of a borohydride fuel cell was initiated by Dr. George Miley and Dr. Nie Luo at NPL Associates, Inc. in Champaign, IL in 2002. Some of the research was conducted at the University of Illinois and was originally aimed at high power density space applications. This project was aimed to develop a fuel cell for Underwater Autonomous Vehicles (UAVs). The objective was to build and demonstrate a high power density 100-watt cell capable of operating for extended times with a power management control system. The cell was built using a new bi-polar plate design and cheaper, easy-to-fabricate materials.

Two types of direct borohydride fuel cells have been reported in literature. These include borohydride/air fuel cells [5–7] and borohydride-hydrogen peroxide [8–10] fuel cells. Typically the two types of cells are further distinguished based on the composition of the membrane electrode assembly (MEA) and catalyst selection. For example, a borohydride-air fuel cell reported by Amendola et al. [7] has attained greater than 60 mW/cm^2 at 70 ^oC. An alkaline direct borohydride – hydrogen peroxide cell utilizing AB_5 and AB_2 alloys was able to achieve 150 mW/cm^2 [9]. Various other direct borohydride-hydrogen peroxide cells have been able to achieve power densities of 50 mW/cm^2 [11] and 130 mW/cm^2 [12]. One of the highest power densities reported has used acidified H_2O_2, with palladium as the anode catalyst and gold as the cathode catalyst. This combination resulted in a power density of 680 mW/cm^2 [13].

A $NaBH_4$ / H_2O_2 fuel cell is composed of several pieces including endplates, diffusion layers, electrodes, catalysts, membrane (PEM) and bipolar plates. The fuel cell employed here is a direct borohydride fuel cell whereby the liquid fuel is directly fed into the cell where the necessary reactions take place. Indirect borohydride fuel cells require a reformer where the fuel

undergoes a reaction with water to produce hydrogen gas which is then pumped to the cell. The direct borohydride fuel cell is advantageous because it requires less ancillary equipment with minimal cell modifications to account for a liquid fuel instead of a gas. Previous work has resulted in the demonstration of a 1 kW cell utilizing a non-optimized bi-polar plate and fuel distribution design. Additionally, more work has been previously conducted in identifying suitable catalysts and various parameters, all of which have been instrumental in the current design, and are discussed later.

The relevant reactions at the anode and cathode, respectively, are as follows:

$$NaBH_4 + H_2O \rightarrow NaBO_2 + 8H^+ + 8e^- \qquad E= 1.776\ V \qquad (3)$$

$$4H_2O_2 + 8H^+ + 8e^- \rightarrow 8H_2O \qquad E= -0.471\ V \qquad (4)$$

Thus the overall reaction is:

$$NaBH_4 + 4H_2O_2 \rightarrow NaBO_2 + 6H_2O \qquad E= 2.247\ V \qquad (5)$$

Although there is additional water used to create aqueous solutions of the sodium borohydride and hydrogen peroxide, it is largely unused and generally not considered a part of the reaction. An overall balance shows that the primary byproducts are sodium metaborate and water. However, in most cases, due to the less than 100% utilization of the hydrogen, some will inevitably exist as a byproduct. Cleary, the theoretical OCV of 2.25 V is much higher than the theoretical voltage of H_2/O_2 cells, which is 1.23 V. The overall fuel cell reactions are depicted in Figure 1 below.

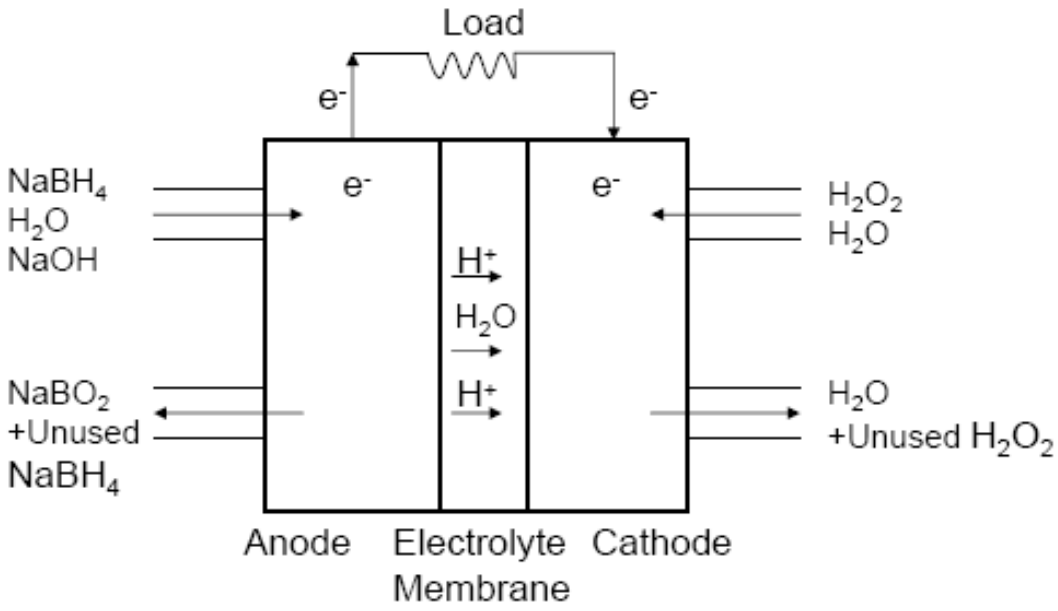

Figure 1: Fuel Cell Basic Operation [16]

1.3 Controls of Fuel Cell Systems

Control systems used with gaseous fuels and liquid fuels need to carefully consider the needs and operating principles of their respective systems. Gaseous fuel cell control systems are generally simpler due to the ease of gas regulation. Figure 2 depicts the components of a hydrogen gas based fuel system.

In this type of system, the gas is compressed and stored in a high pressure cylinder. A pressure regulator is used to decrease the incoming pressure to that necessary for the fuel cell. Typically, most hydrogen gas based systems have between one to three passes of reactants through the fuel cell. The fuel is introduced to the fuel cell by opening a solenoid which allows a flow from the high pressure region to the low pressure (atmospheric region). Once the fuel cell channel volume has been filled, the solenoid is closed to allow the fuel to react with the catalyst. In the case of hydrogen-air fuel cell systems, only the valuable hydrogen feed is controlled by a

solenoid. The cathode side is subjected to a continuous stream of air due to the need of waste heat and water vapor removal. The continuous blowing of air across the cathode is also beneficial to fuel cell performance because the oxidation is rate limiting. On the anode, the hydrogen is decomposed into protons across the catalyst. The solenoid remains closed until a prescribed hydrogen concentration is reached for the required power level. Alternatively, the hydrogen is recirculated until it is sufficiently utilized. At this point, the solenoid reopens to allow fresh hydrogen to enter the cell stack, and the process repeats. Thus in the case of such a gas fuel cell, the control of the fuel feed is primarily obtained through a simple solenoid actuation process which is determined by the fuel concentration and power needs [14].

On the contrary, a liquid based fuel cell almost always requires a recirculation loop. Unless stored at a high pressure, a pump is required to distribute the liquid. In many cases, this is logistically simpler and more energy efficient than using high pressures. However, there is a significant disadvantage in that pumps cannot be actuated quickly in the same manner as a solenoid. In fact, depending on the type of pump, operating a pump in this way can be extremely detrimental to its performance and lifetime.

In the case of the borohydride fuel cell, there are further disadvantages to using a stop–start type of control system. Firstly, according to equation (5), one of the main byproducts of the anode reaction is sodium metaborate ($NaBO_2$) which is a solid under normal room conditions. Although this byproduct is soluble in water, there is a potential for it to condense out of the solution at lower temperatures. If allowed to condense, the metaborate would clog the carbon cloth electrode and reduce the active area which then resulted in lower cell performance. Secondly, the decomposition of sodium borohydride over the palladium catalyst [15] leads to generation of gases which can result to an unsafe buildup of pressure. Although this is less of a

concern on the cathode side, there is still some gas generation due to the decomposition of hydrogen peroxide on the gold catalyst. However, gold has been shown to be significantly better at directly reducing hydrogen peroxide [16]. Such a buildup of gas can cause an undesired and detrimental stress on the cell components and is a potential explosion hazard. Therefore, it is vital that this gas is released from the cell as it is generated. A one-pass-through or closed-loop system utilizing a solenoid would not allow for this.

The exothermic nature of the reactions means that heat is generated as a product. As the fuel cell heats up, the cell performance increases. However, after certain temperatures, the Nafion membrane and carbon cloth electrodes will be susceptible to degradation [17]. Therefore, it is vital to remove heat from the system as well. In the case of this fuel cell, the bipolar plates are constructed of a stainless steel separation layer (discussed in section 3) and stainless steel channels. This construction is conducive to heat transfer and heat generated at the anode can be transferred to the cathode. If only heat transfer is considered, it would be adequate to have a continuous flow across either only the anode or cathode. However, because of the gas generation reasons mentioned above, this is not advisable.

It becomes clear that a recirculation of the fuel and oxidizer is needed. It is important to note that when the fuel or oxidizer is re-circulated, each pass through slowly decreases the overall concentration. During fuel cell operation, the maximum possible power generation will slowly decrease due to the reduced overall concentration. This is opposite to the once-pass-through systems which introduce fresh fuel in each cycle and are therefore able to achieve maximum stack power at all times. This typically also results in better fuel utilization for hydrogen gas systems.

CHAPTER 2: DESIGN OF DIRECT BOROHYDRIDE FUEL CELL

2.1 General Design Considerations

The design of the bipolar plate is of vital importance to the performance characteristics of the fuel cell. There are several important features that a bipolar plate needs in order to function properly. A bipolar plate is the backbone of any fuel cell stack, and has several important purposes. The plate distributes the fuel and oxidizer evenly across its surface via the use of channels. The reactant then comes into contact with a catalyst layer where the reactions occur and generate electrons in addition to other products. In any fuel cell, electricity is generated through the transfer of electrons from the anode to the cathode or vice versa. Therefore, the bipolar plate needs to be electrically conductive [18]. In the case of borohydride or hydrogen fuel cells, the electrons generated on the anode of the bipolar plate need to be transferred across to the cathode where the reduction reaction occurs.

Depending on the application, there are several design options which need to be taken under consideration. These include material selection, channel design, sizing, cost, and manufacturability, to name a few. When a fuel cell stack is assembled, several bipolar plates are connected in series and tightly fastened such that there are no leaks at the interface of the membrane electrode assembly (MEA) and the bipolar plate. As a result, plate material cannot be too soft and needs adequate strength to withstand the fastening pressures. In addition to electrical conductivity, it is also beneficial for the plates to have good thermal conduction [18]. Good thermal conductivity aids in heat removal from the cell and also avoids local hotspots which can, over time, cause premature failure.

2.2 Fuel Cell Structure and Assembly

The bipolar plates used in this fuel cell are unique in that they are constructed from two separate materials. Traditional plates are often manufactured from only graphite which acts both to distribute fuel and conduct electricity. Some advantages to using these plates include ease of machining, low contact resistance, and excellent corrosion resistance. However, a major drawback of graphite plates is that the machining process is expensive. Furthermore, the brittle nature of graphite means that the plates need to be thick and handled with care. By increasing the thickness, the contact resistance also increases, which is detrimental to the fuel cell [19]. Figure 2 shows an example of a graphite bipolar plate used in hydrogen-based fuel cells.

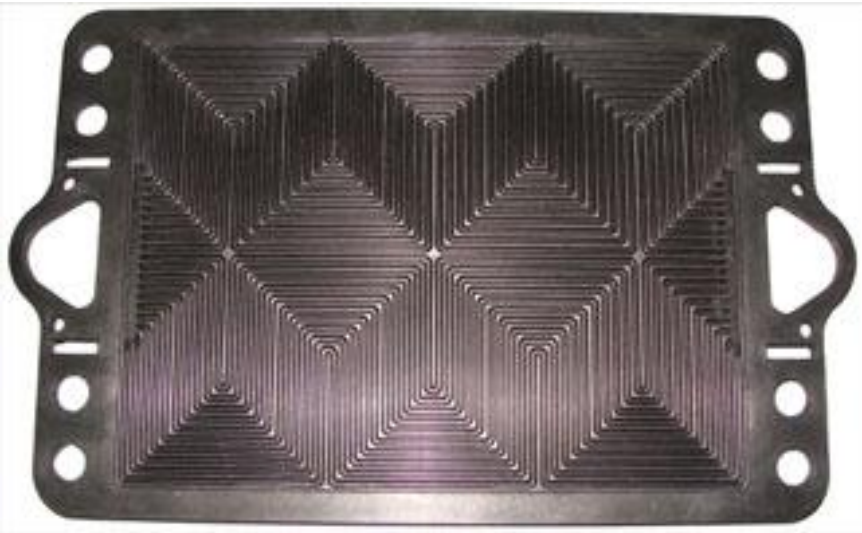

Figure 2: Graphite Bipolar Plate [20]

In hydrogen gas based systems, where the reactants do not typically react at ambient conditions or unless a catalyst is present, a single material plate is adequate. However, in this direct borohydride fuel cell, the fuel and oxidizer undergo a violent exothermic reaction when mixed. Therefore, it is imperative to ensure that the two are kept separate. In a graphite bipolar

plate with an integrated manifold design, which is commonly used with hydrogen/air fuel cells, leakage does not pose a huge problem. The graphite plates are often injected with a resin to prevent hydrogen diffusion through the plates [18]. However, if a single material-integrated graphite manifold design was used with a liquid fuel cell, adjacent cells would experience shorting and violent reactions could potentially cause rapid heat buildup. A previous version of the direct borohydride fuel cell developed at the University of Illinois utilized graphite bipolar plates but did not have an integrated manifold design. Instead, the novel manifold design supplied the fuel to each oxidizer plate separately. One objective of the current design was to develop an integrated manifold design to reduce complexity of the pumping system, weight, and associated balance-of-plant components. To the author's knowledge, this bipolar manifold design is the first being demonstrated with a direct borohydride fuel cell.

Figure 3 shows the original design of the bipolar plate. One important feature of this plate was that the flow channel manifold is made from an electrically resistive material while the main flow section of the plate is composed of stainless steel. It is vital to have this distinction because a short can easily be caused within the cell, which could cause decomposition of the fuel and oxidizer. As seen, the bipolar plate is composed of several different layers of materials.

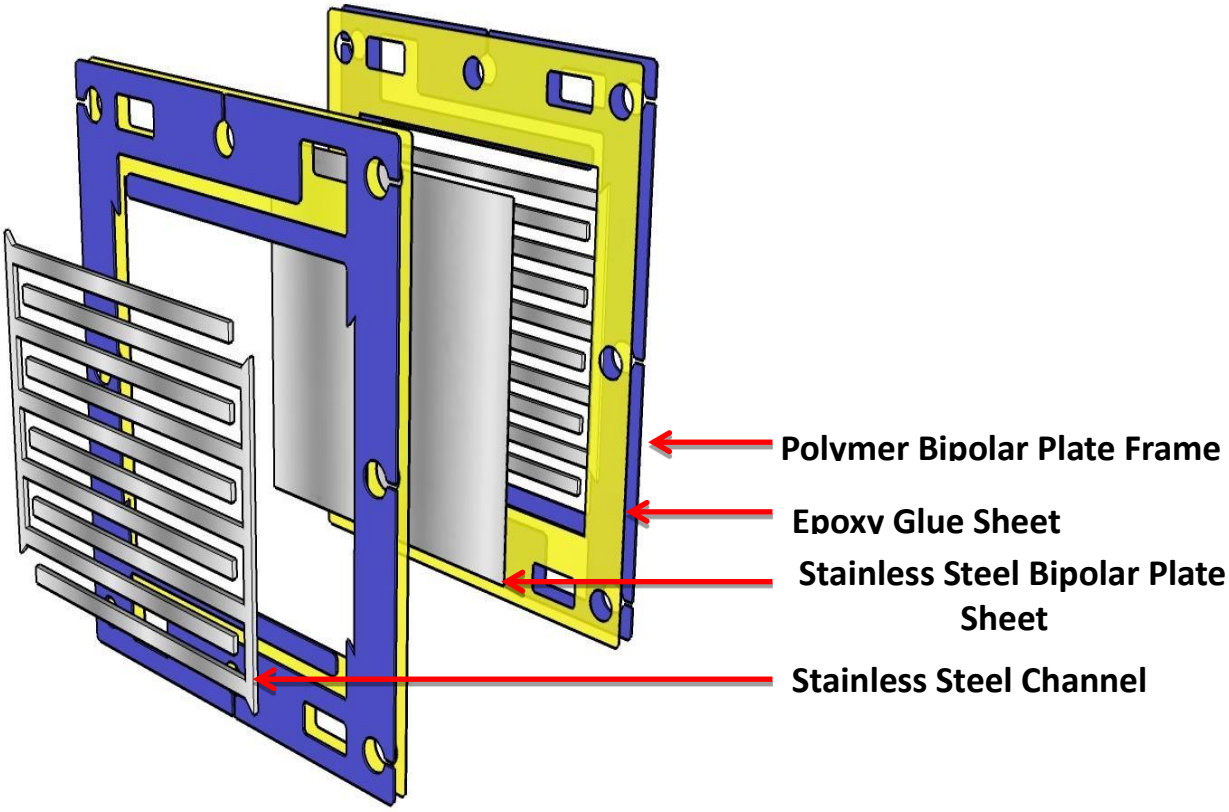

Figure 3: Design of Bipolar Plate [21]

The main structure of the cell consists of a polymer plate. This blue material is a polymer composite which provides excellent durability, machinability, and strength. The holes and channels were machined using water jet cutting. A thin sheet of stainless steel was sandwiched between two of these plates. Using stainless steel channels, the components were affixed using epoxy sheets in a high temperature baking process at a pressure of 5,000 psi. The thin sheet of steel was used to provide low electrical resistance between the two sides of the bipolar plate and as a support for the stainless steel channels. The plates have small openings in order to transfer the fuel and oxidizer to the channels. Figure 4 shows the actual manufactured plates.

Figure 4: Manufactured Bipolar Plates [21]

In order to assemble the complete fuel cell, two end plates were also manufactured. The end plates are very similar to the bipolar plates except that they have a flow path only on one side. One end plate is used as the last anode, whereas the other is used as the last cathode. The end plates also function as the inlets and outlets for the fuel and oxidizer. As seen, each end plate is manufactured in a similar manner to the bipolar plate. Using a polymer as the base material, the stainless steel channels were again affixed using epoxy sheets at a high temperature baking process. Holes were then drilled and tapped to allow for plugs and fuel distribution nozzles.

From previous designs and experience, the 100 watt requirement of the fuel cell meant that at least a 10 cell stack is required, which translates to nine bipolar plates and the two endplates. However, to be safe a 14 cell stack was constructed. On one side of the bipolar plate, the relevant electrode layer was added which contained the catalysts. A Nafion 115 membrane was added using rubber gaskets to ensure a leak free seal. A second electrode was then added followed by another bipolar plate. The two electrodes and a Nafion membrane are referred to as the MEA. In this manner, the whole cell was assembled and bound by simple bolts and nuts. The electrode layers consisted of a carbon cloth with the relevant catalysts implanted within. Figures 5, 6, and 7 show the assembly view of the stack, a partially assembled stack and a completely assembled stack, respectively.

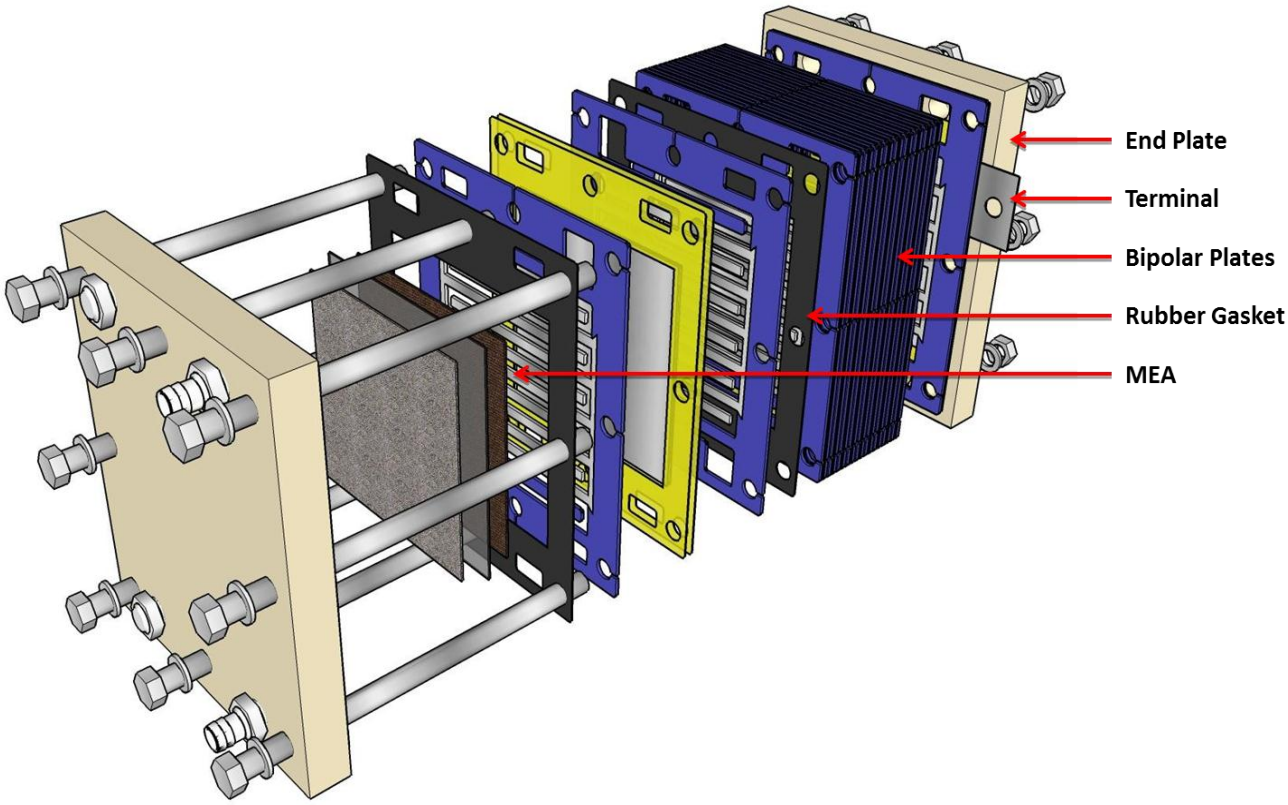

Figure 5: Assembly View of Stack [21]

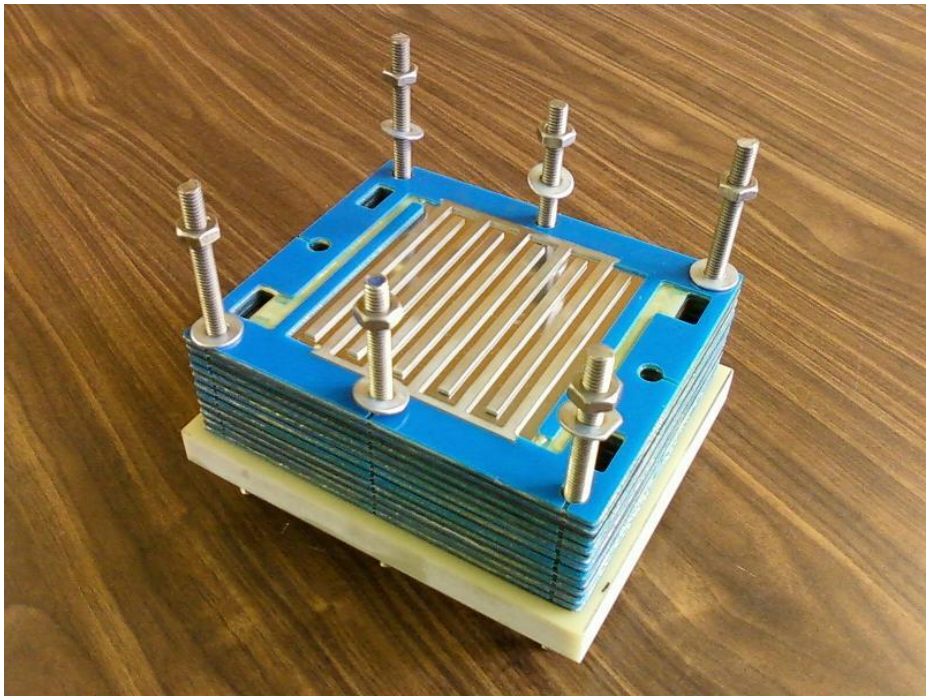

Figure 6: Partially Assembled Stack

Figure 7: Fully Assembled Stack

2.3 Catalyst and Membrane Selection

The selection of the anode and cathode catalyst is extremely vital to the successful operation of the fuel cell. Previous research shows that palladium is effective for the anode oxidation reaction [22]. On the cathode side, gold has been shown as the ideal catalyst for the hydrogen peroxide oxidation reaction [16]. The catalysts were obtained in power form and deposited onto carbon cloth layers. The anode catalyst layer required electrodeposition of Palladium Chloride (II) whereas the cathode carbon cloths were simply dipped into the Gold Sodium Dichloride ($AuNaCl_4$) – water solution. Depending on the various parameters, different amounts of catalyst would have been deposited. The deposition amounts and exact surface composition was not studied since it was assumed that there was sufficient coverage.

The selection of an appropriate Nafion membrane also plays a role in the performance of the fuel cell. Nafion is fragile and easily susceptible to tearing and/or degradation in the presence of high temperatures. For this reasons, a thicker Nafion membrane will make the cell more stable and flexible. However, a thicker membrane also causes increased contact resistance, which is unfavorable. Therefore the selection of the most suitable membrane is a tradeoff between stability and contact resistance of the cell. For this fuel cell, a 127-μm thick Nafion 115 membrane was used because previous experience has shown that it can withstand corrosion from the fuel and oxidizer as well as the expected temperature levels within the stack.

2.4 Testing Setup

The testing setup (Figure 8) used to determine the performance of the cell was relatively simple. It was composed of the fuel cell, two beakers containing the fuel and oxidizer, a 4-channel laboratory pump capable of flow rates up to 166 ml/min and a DC load bank. The pump

was used to circulate the fuel and oxidizer, while the load bank was used to vary current. For each current, the relevant voltage was recorded. The power was obtained by multiplying the voltage and current.

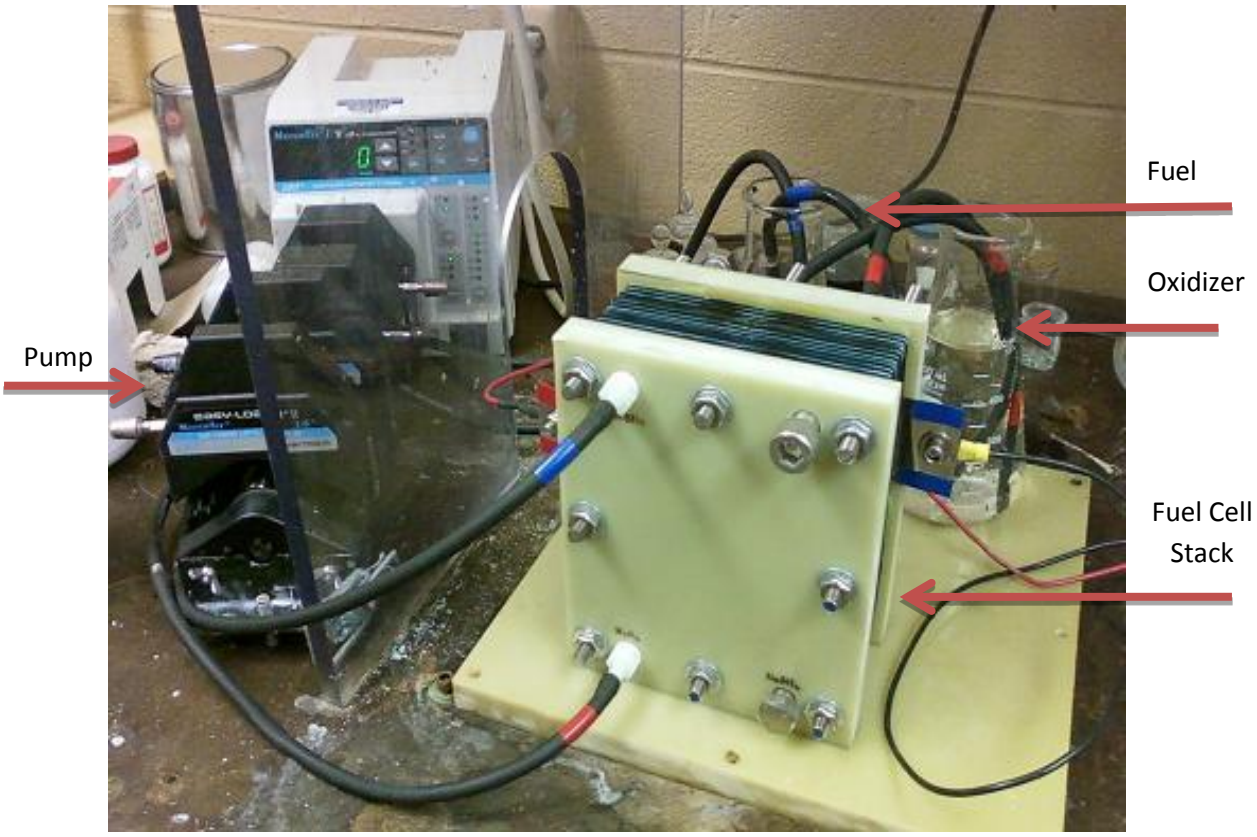

Figure 8: Test Setup

CHAPTER 3: TESTING AND RESULTS

3.1 Testing of First Cell Stack

The first fuel cell, which was designed and built in the above discussed manner, attained a maximum power level of 140 mW/cm^2 or 169 W for the complete 12 cell stack. The power curve for this fuel cell stack is provided below in Figure 9. This power density is similar to those reported in previously mentioned literature [5-10].

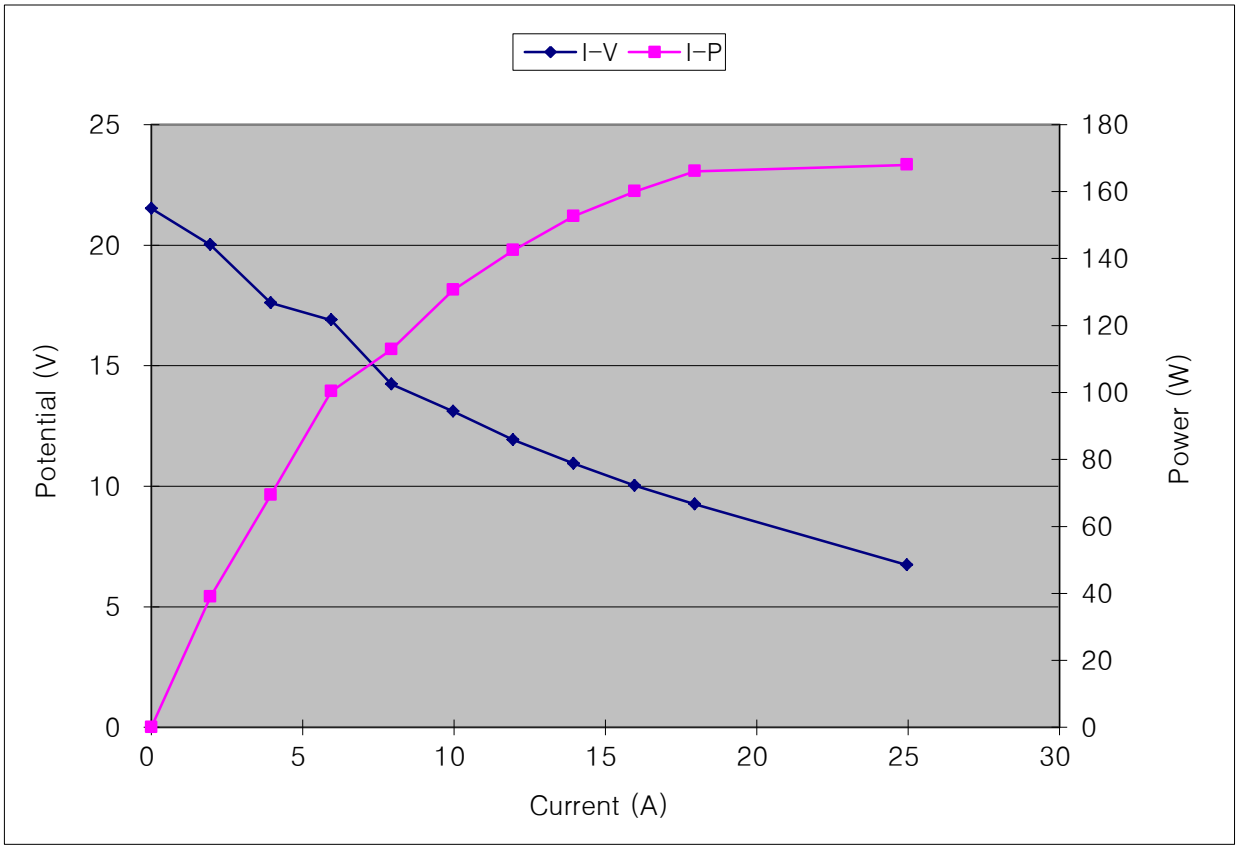

Figure 9: Performance of First Cell Stack

During operation of the stack it was observed that the fuel, which is usually clear or slightly opaque, became extremely dark. Furthermore, there seemed to also be a high amount of gas generation in both the anode and cathode sides of the stack. This gas generation rate was much higher than seen in previously developed fuel cells. For this first test, the fuel cell was run for approximately 20 minutes without any noticeable power loss or cell degradation.

A few days later, a second test on this same cell stack did not achieve the previous power levels. Since the cell was not disassembled within that time period, it was assumed that part of the reason for decreased cell performance could be wash-out of the catalyst. Because the anode catalyst is palladium chloride (II), this could also explain the black color of the fuel after being circulated through the fuel cell. By allowing the spent fuel to cool, it becomes evident that the blackening is due to small, micron-scale suspended particles. Although explicit testing was not conducted on the composition of the fuel, it was assumed that these particles were palladium.

Based on this assumption, an in-situ electroplating procedure was done to coat catalysts back onto the carbon cloth layers. The in-situ electroplating is extremely convenient as it does not require disassembly of the fuel cell. A palladium solution was prepared for both the anode and cathode of the fuel cell. The solution was then pumped through the anode while applying a small voltage and current. This method allows electrodeposition onto the carbon cloth. The same procedure was then conducted for the cathode side. Although gold is a more suitable catalyst for the cathode, previous experience has shown that palladium is still effective. Although the palladium participates in the cathode reduction reaction, it also increases the oxygen gas generation rate [16]. This unwanted side-effect introduces additional pressure to the system while increasing the depletion rate of the oxidizer due to the hydrogen generation.

Once the electrodeposition process was complete on both sides, a test was then carried out. Unfortunately, this test did not produce the expected power levels which were achieved in the first test. Because the cell performance was not adequate, the results implied that washout of the catalysts was not the cause of the problem. The black coloration of the fuel and the excessive gas generation can be explained by another hypothesis. Internal leaking within the cell can cause crossover of the fuel to the cathode side and/or crossover of the oxidizer to the anode side. Because the reaction between the fuel and oxidizer is exothermic and relatively violent, even a small amount of crossover can have drastic effects. Proof of this phenomenon was found after the bipolar plates were disassembled. Generally, the fuel and/or oxidizer should only enter one side of each bipolar plate. However, as Figures 10 and 11 show, there are clear flow marks on both channels. This implies that there is crossover within the plate.

Figure 10: Flow Marks on Side 1

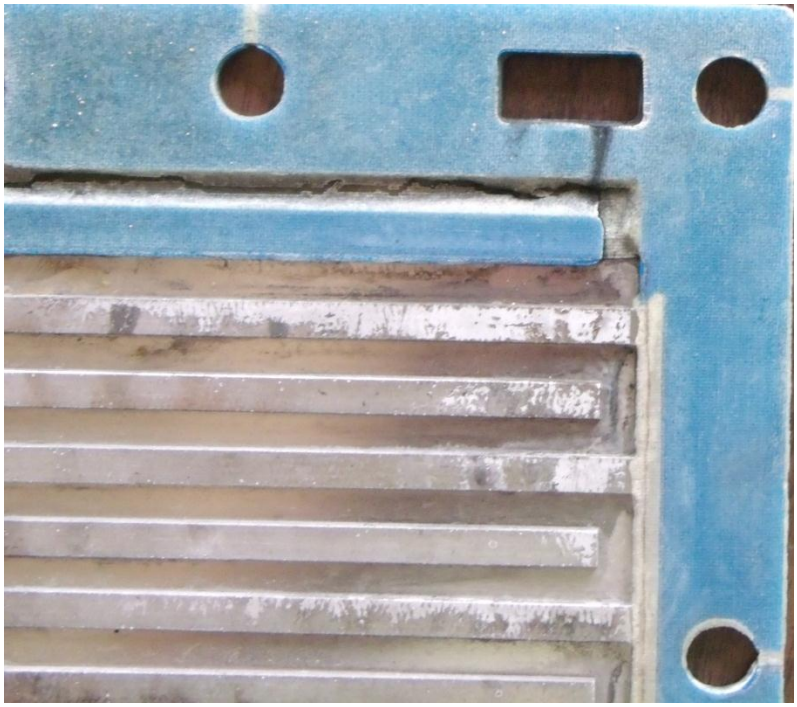

Figure 11: Flow Marks on Side 2

Another reason for poor cell performance could be inadequate flow to the channels. When the fuel cell stack was disassembled, there were additional flow marks on the thin steel sheet, part of the bipolar plate. In a proper flow, the fuel and/or oxidizer should very closely follow the serpentine stainless steel channel patterns. This commonly used flow pattern allows good utilization of the fuel per pass while simultaneously yielding good power density [23]. The flow marks seen in the channels, however, indicated that the fuel flow does not follow the serpentine path. The flow pattern simply enters the channel and flows straight down to the bottom via a path under the stainless steel channels. In fact, the path indicates that roughly only 10% of the available flow area was utilized. This does not mean, however, that only 10% of the available power density is achieved. The diffusion carbon layer allow for better distribution of the reactants.

Although there was no indication of such a flow path occurring on the cathode side, the flow path is also the same on the other side of the cell. To confirm this, the directions of the bipolar plates were reversed. A test was run and visible marks, similar to earlier results, were discovered. This showed that the issue of inadequate fuel flow affects both sides of the bipolar plates.

During the high temperature process which attaches the stainless steel channels to the bipolar plate, the channels change shape. Because the cooling process is uneven, the channels become slightly warped. The deformed channels do no lie flat against the steel sheet, which results in a poor flow path. Figure 12 shows the stainless steel channels after they undergo the high temperature process. Clearly, the channels are no longer lie flat and are deformed.

Figure 12: Deformed Stainless Steel Channels

Ideally, the channels should be spot welded to the plate in multiple locations. However, Because the stack was producing enough power, and due to time concerns, this solution was not implemented. The black discoloration could also be caused due to internal mixing. A high gas and heat production rate is further evidence that the two reactants are mixing. Because there appeared to be black discoloration only in the anode, it was evident that the oxidizer was crossing over to the anode in the stack.

The reason for the crossover was determined to be the flexibility of the rubber gaskets. When the fuel cell is assembled, the rubber gaskets are compressed and supported by the bipolar plates. However, there is no support for the gasket in the channel openings. While liquid fuel is being pumped, and in the presence of heat, the rubber gasket becomes even more flexible and deforms. This allows the flow to enter both sides of the plate. The solution, therefore, is to provide a rigid backing for two channels on each side of the bipolar plate. These two channels are the ones which don't require a flow.

In order to combat the issue, a layer of epoxy was first added to the plates. To ensure that the epoxy would not "melt" into the channel gap, a small Teflon backing layer was added to support the epoxy during the heating process and then later removed. A five cell stack was again put through a test. However, as the test progressed, there were elevated levels of gas and heat. The stack was disassembled, and showed similar signs indicating crossover. The normally rigid epoxy had deformed and no longer provided a leak-proof seal between each successive bipolar plate. Figure 13 shows the sheets of epoxy which are deformed around the channel area.

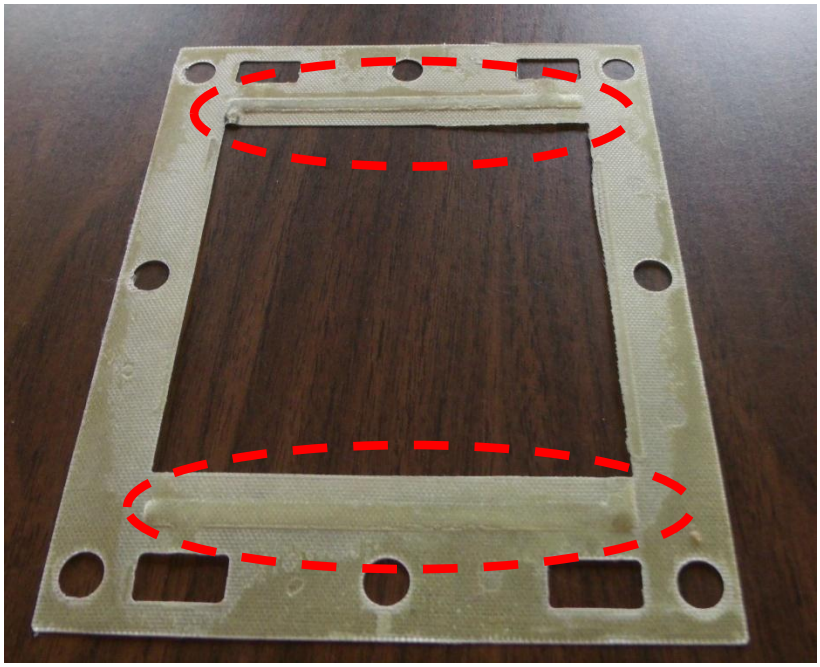

Figure 13: Deformed Channel Area in Epoxy Sheet

An alternative solution in the form of Teflon sheets was sought as a fix to the leaking channels. Teflon sheets were used as gasket material instead of rubber and a test of a 2 cell stack showed no issues with internal mixing. However, a larger 10 cell stack again showed signs of leaking from the cells. This is because a larger stack size produces more heat which cannot be dissipated as quickly as the two cell stack. Therefore, the heating causes deformation of the Teflon sheets and can be attributed to the changes seen in the epoxy sheets.

3.2 Modifications to First Cell Stack

To make the required changes, it was necessary to add a second polymer plate to each side of the existing bipolar plates. These new “cover plates” consisted of support for both channels and were also intended to block any flow entering those channels as well (Figure 14).

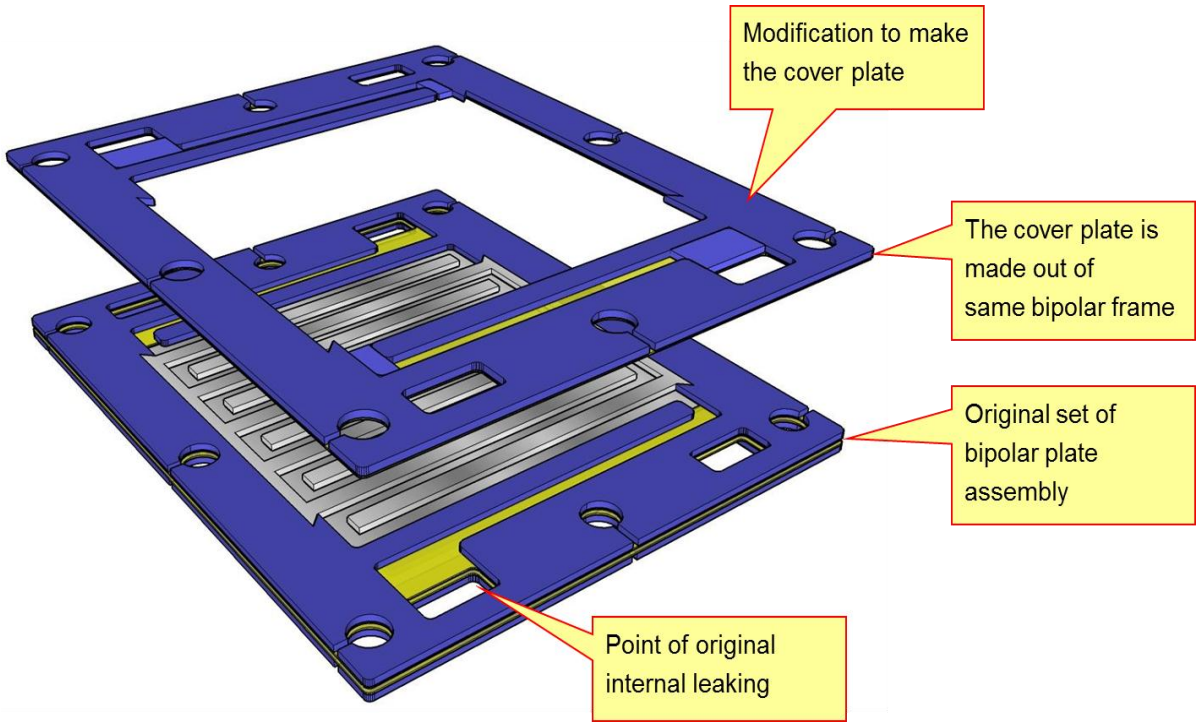

Figure 14: Design modifications [21]

3.3 Testing and Further Modifications to Second Stack

As before, the cover plates were attached via epoxy sheets. As a result of these modifications, the thickness of the bipolar plates increased to twice the original design. This is shown in Figure 15.

In order to compensate for the gap between the channels and the membrane, a filler material was needed to both support the catalyst layer as well as provide an electrical pathway. A thin layer of carbon felt was used for this purpose, shown in Figure 16. Although carbon felt is electrically conductive, it has a higher resistance than the single carbon cloth layer present in the original design.

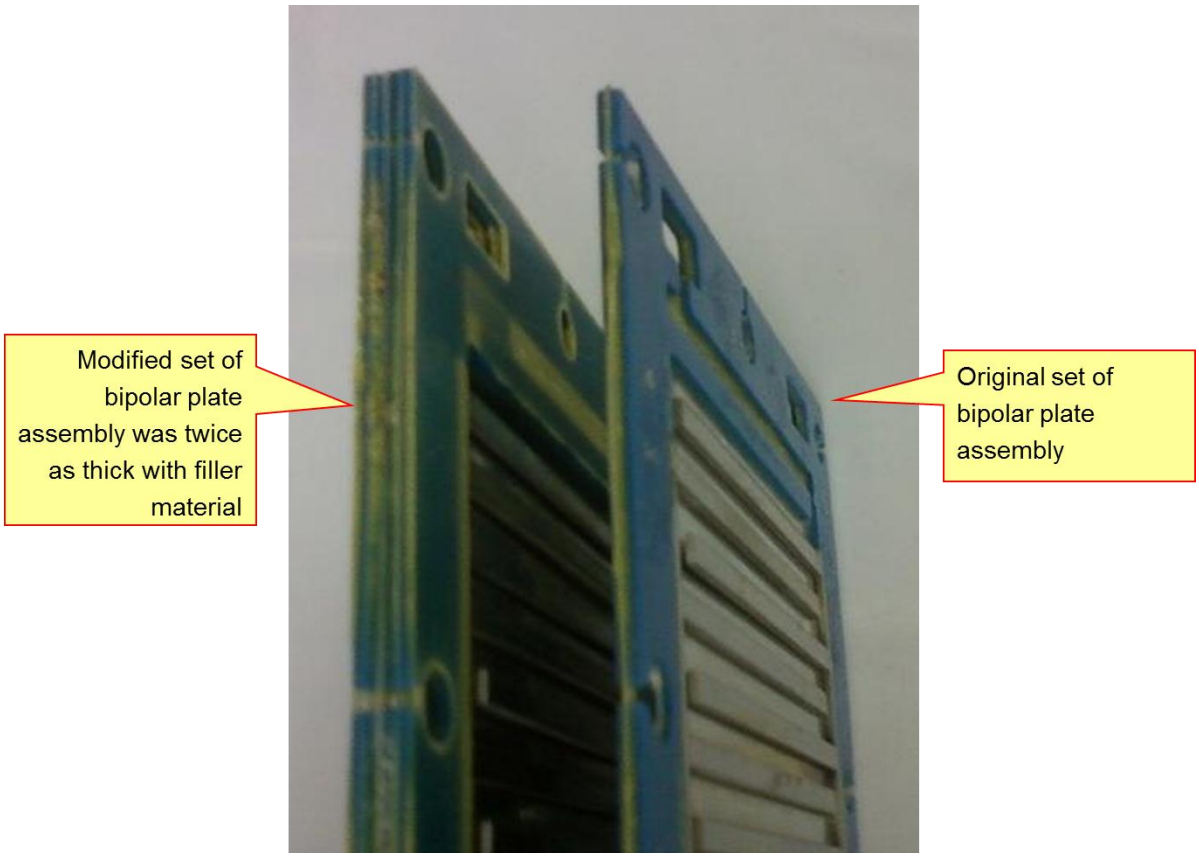

Figure 15: Actual modified plate [21]

Therefore, a slightly lower cell performance was expected using this filler material. However, tests conducted using this material showed severely degraded cell performance. Both Teflon and rubber gaskets were tried, with neither having a positive effect on the cell.

The carbon felt was then replaced with nickel foam sheets on both sides of the cell. Nickel foam provides a more rigid support layer and has a much lower electrical resistance compared to the felt. Although the test results showed a power density of 140 mW/cm^2, there were still high amounts of gas generation and black discoloration of the fuel. Furthermore, over the duration of the test, the hydrogen peroxide solution slowly turned a turquoise/green color. In a normal cell, this discoloration should not occur in the cathode. The only difference between this test and previous efforts was the addition of the nickel layers instead of the carbon felt. This indicates that a side reaction occurs in the nickel foam causing discoloration of the peroxide.

Figure 16: Carbon Felt Filler

Although specific tests were not conducted, the turquoise compound is most likely due to nickel sulfate. A color similar to that shown in Figure 17 was observed.

Figure 17: Color of Peroxide Solution Post Testing [24]

The formation of this product can also cause heat generation as well as decomposition of the peroxide which in turn leads to a lower energy density of the system. Although the decomposition was more prominent in the cathode side, the sodium borohydride is also subject

to the similar effects at the anode. According to its Material Safety Data Sheet (MSDS), sodium borohydride is reactive to transition metals and can undergo a decay process in their presence. Visual evidence of such a phenomenon in the borohydride was not present.

Nevertheless, there was some evidence that the aforementioned decomposition was occurring on both sides of the cells. As the cell underwent several tests, the thickness of the nickel foam began slowly decreasing. Although the initial compression is due to the assembly of the stack, the foam became significantly thinner over time. Figure 18 shows the degraded nickel foam after the tests. This reduction in thickness was noticeable on both the anode and cathode foams indicating that side reactions were occurring, causing gradual decomposition of the foam. The individual anode and cathode thicknesses were not tested and thus there is no information on the rate of foam removal.

Figure 18: Nickel Foam Degradation

To counter this issue, the cathode nickel foam layer was replaced with an additional stainless steel channel layer. This was done to still allow for adequate contact between the

various layers of the cell while simultaneously preventing decomposition of the hydrogen peroxide. Using a spot welder, the stainless steel channels were welded to the cathode side of the existing bipolar plates. A 2 cell test showed decreased cell performance over the desired 14 W/cell test.

One explanation for this can be found in the increased thickness of the channels. Because the channel volume was essentially doubled, the fluid layer would not be thick enough to come into contact with the carbon cloth/catalyst layer. A 2 cell test utilizing this setup did not yield an adequate power level. In this case, the end plates did not have a double channel layer, but instead had one nickel foam layer. A channel was then added to the cathode end plate instead of the foam layer. This double channel setup did not seem to produce the required power levels, either. Adding stainless steel channels to the stack was determined to not have any effect on its output.

After these unsuccessful tests stainless steel channels, a decision was made to use the control system. By using the control system with the fuel cell, the team could determine if the overall system performance is enhanced or hindered. Because the pumping flow rate of the system was higher than that of the experimental pump used in Figure 8, the performance of the fuel cell was expected to increase.

In order to do this, however, the original stack with the nickel foam had to be reassembled because it had produced the desired power level. Upon reassembly, using one layer of nickel foam on the cathode and anode, a 2 cell test was conducted. This test, however, did not achieve the original power level. In an attempt to correct this issue, the stack was laid in a horizontal position. This position of the stack would allow the stack to fill up from top to bottom and allow all of the fuel/oxidizer to come into contact with the catalyst layer. Because the

cathode reaction is the limiting reaction of the system, it is crucial that the oxidizer is more readily accessible to the cathode catalyst layer. Nevertheless, the anode layer is also exposed to an increased flow of fuel. This setup achieved the 140 mW/cell power output. This originally indicated that the horizontal setup is more effective at distributing the fuel over the internal channel area.

However, when a larger cell stack was assembled, the fuel cell did not achieve this power density. This was most likely due to the compression of the nickel foam layers which led to inadequate surface contact between the channels, foam, and electrode layers and thus increased the contact resistance while reducing cell performance.

In this configuration, the cell was placed horizontally which had previously yielded good results. Because the nickel foam layer was suspected as the reason for the degradation in performance, an additional nickel foam layer was added to both the anode and cathode sides of the stack to counter any issue with high contact resistance. The additional nickel foam layer did not help and the 10-cell stack was only able to produce a maximum of 50 W, shown in Figure 19 below.

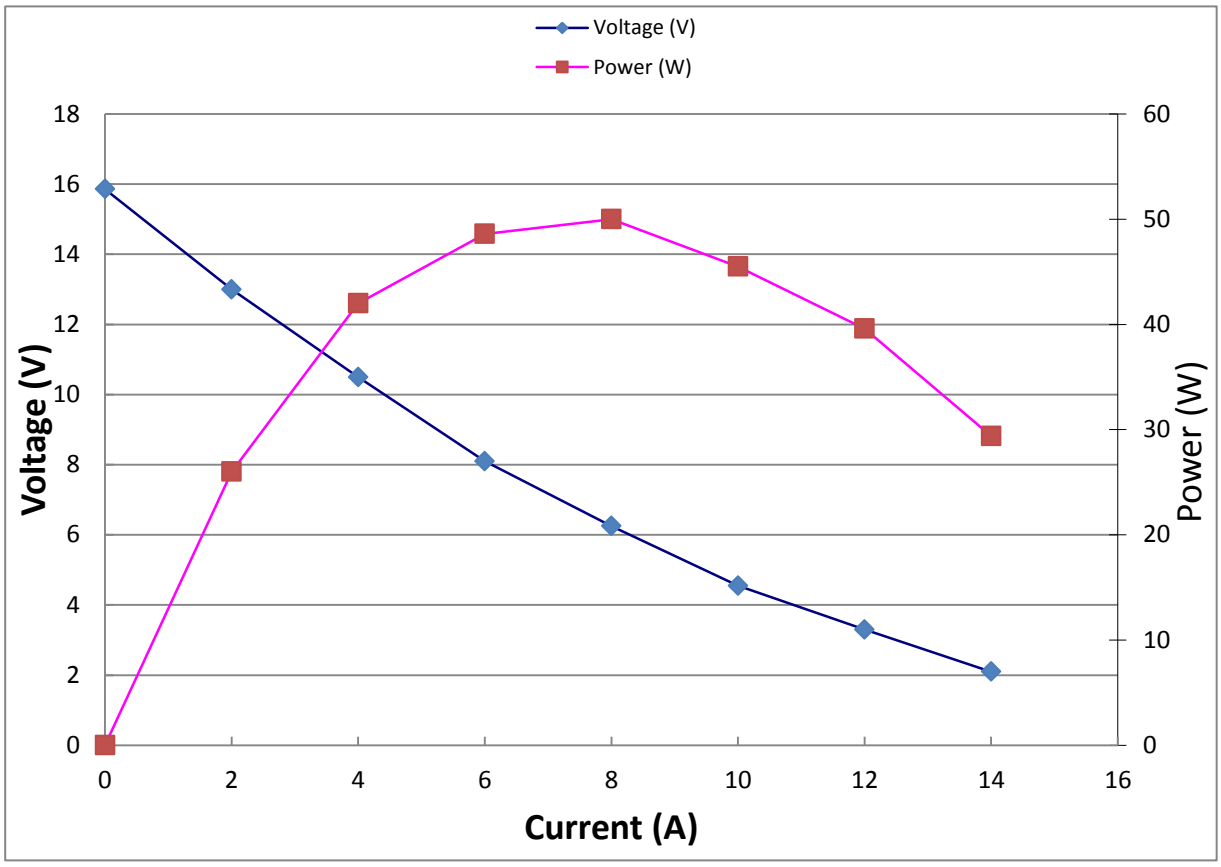

Figure 19: Second Stack Performance

3.4 Leak Testing

The inconsistency between this result and previous tests indicate that something else was causing deterioration within the stack. Based on the severity of the gas generation, it is safe to assume this was due to crossover which could also cause a short within the stack. Between each of these tests, and when the stack was disassembled and reassembled, a leak test was conducted to check for any crossover within the cell.

The leak test consisted of submerging the fuel cell in water. Then, using some tubing, air was blown through the inlet of the fuel channel while the exit of the fuel and oxidizer channels was blocked. If there was any internal leaking within the cell, bubbles would be seen escaping from the inlet of the oxidizer channel. Once one side of the fuel cell underwent this test, the opposite side was exposed to the same procedure. In other words, the inlets of the fuel and

oxidizer channels were closed while the exit of the fuel channel was left open. Meanwhile, air was blown through the exit port of the oxidizer.

If any of these tests showed signs of leaking, the cell was disassembled. Then, each bipolar plate was reassembled one by one to determine which bipolar plate was the cause of the leaking. Of course, any other issues which contributed to leaking such as torn membranes, faulty gaskets, etc. were corrected as well. Although the leak test was not originally used, most experiments using the "thicker" bipolar plates did use the test. The leak test proved extremely useful in identifying faulty bipolar plates.

A goal of the leak test was to identify these faulty plates and remove/repair them before running a test with fuel and oxidizer. If a faulty plate is left within the stack, internal mixing causes undesired heat and gas generation, which can potentially damage other bipolar plates within the stack. Although the leak test may have been partially successful at avoiding this, it did not completely prevent damage of the plates. In several tests, a pre-experiment leak test showed no internal leaks within the stack. However, after the experiment, a leak test would show leaking. This indicates that the leaking was created during the experiment.

Because the leak test involved a person blowing air through the stack, the associated pressure was not very high. However, reactions at the anode and cathode while the fuel cell was running could cause a buildup of pressure which is higher than the leak test pressure. This higher pressure can induce a failure in one plate which results in small amounts of internal mixing. Then, the pressure buildup affects other plates and causes a cascading effect. During experiments, it was visually evident that the pressure within the stack was much higher than that

used in the leak tests. By adding pressure relief vents, as discussed in the recommendations section, this issue can potentially be avoided.

CHAPTER 4: CONTROL SYSTEM OF FUEL CELL

4.1 Control System Objectives

As mentioned earlier, the design of a control system for a borohydride fuel cell is especially challenging given the liquid nature of the fuel and sometimes gaseous byproducts. This fuel cell was developed for an Underwater Autonomous Vehicle (UAV). Because air is not readily available, a hydrogen/air fuel cell is not a viable option. Although hydrogen/oxygen fuel cells could potentially meet power requirements, storing them under pressure requires large space and adds unnecessary weight to the vehicle. A sodium borohyride/hydrogen peroxide fuel cell offers excellent power and energy density and is ideal for this application. There is no need for high pressure tanks and the liquid fuel and oxidizer are easy to handle and non-toxic.

The control system developed for this purpose had several main objectives:

1) The whole system was to run on a nominal 12 V DC.
2) A battery will be used for initial fuel cell startup. Then, the fuel cell will provide power for the control system and prescribed loads.
3) The control system will monitor fuel cell voltage and automatically start/shut system down requiring only an initial user input.
4) The balance of plant (BOP) will allow safe fuel cell operation while employing the best strategy to minimize fuel and oxidizer consumption.
5) The voltage from the fuel cell shall be regulated to allow for some fluctuations.

4.2 Components and Original Control Algorithm

The control system has a relatively simple algorithm which allows the fuel cell to startup, monitor its performance, and shut down once the cell loses its potential. Figure 20 shows the main controller and Figure 21 shows the original design for the balance of plant and electrical components for the fuel cell. The final prototype of the system closely matches this design with some changes which will be discussed later. First, however, the original intent of the system will be described. Because the fuel and oxidizer sides of the system are identical, only the fuel side will be discussed with operation on the oxidizer being exactly the same.

A 12 V DC, 4.5Ah Lithium Ion battery was chosen to be used for the initial startup of the fuel cell. Upon user input, the system would power the fuel pump the solenoid valve from the sodium borohydride tank. The solenoid valve going into the tank is kept closed. This would allow the fuel to circulate through the fuel cell and fill the recirculation loop consisting of the mixer, pump, and fuel cell stack. An identical process occurs on the oxidizer side of the system. At this point, both the fuel and oxidizer are passing through the stack, resulting in power production. The voltage of the fuel cell increases until the desired operating voltage is reached.

The controller module continuously monitors this voltage until a preset point is reached. At this operating voltage, the controller module then transfers all components to draw power from the fuel cell instead of the battery. As the fuel cell is loaded and its voltage drops, the regulator is turned on and functions to keep the voltage steady. A 150 Watt DC-DC converter capable of accepting input voltages from 9–14 V was chosen for this purpose. The converter regulates the output to 13.8 V through Pulse Width Modulation (PWM). Power generated from

the fuel cell is used to power the control system, an external load, and charge the battery via the charging controller.

The controller module, shown in Figure 20, is composed of a micro controller which monitors all relevant inputs and outputs. The second part of the module consists of relays and other power distribution electronics.

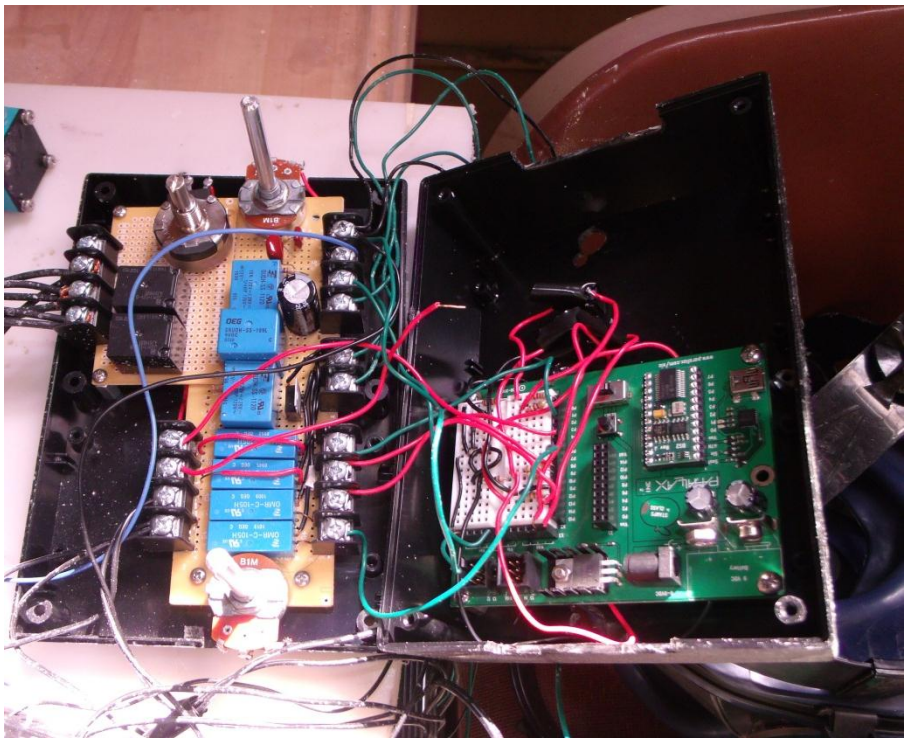

Figure 20: Controller Module

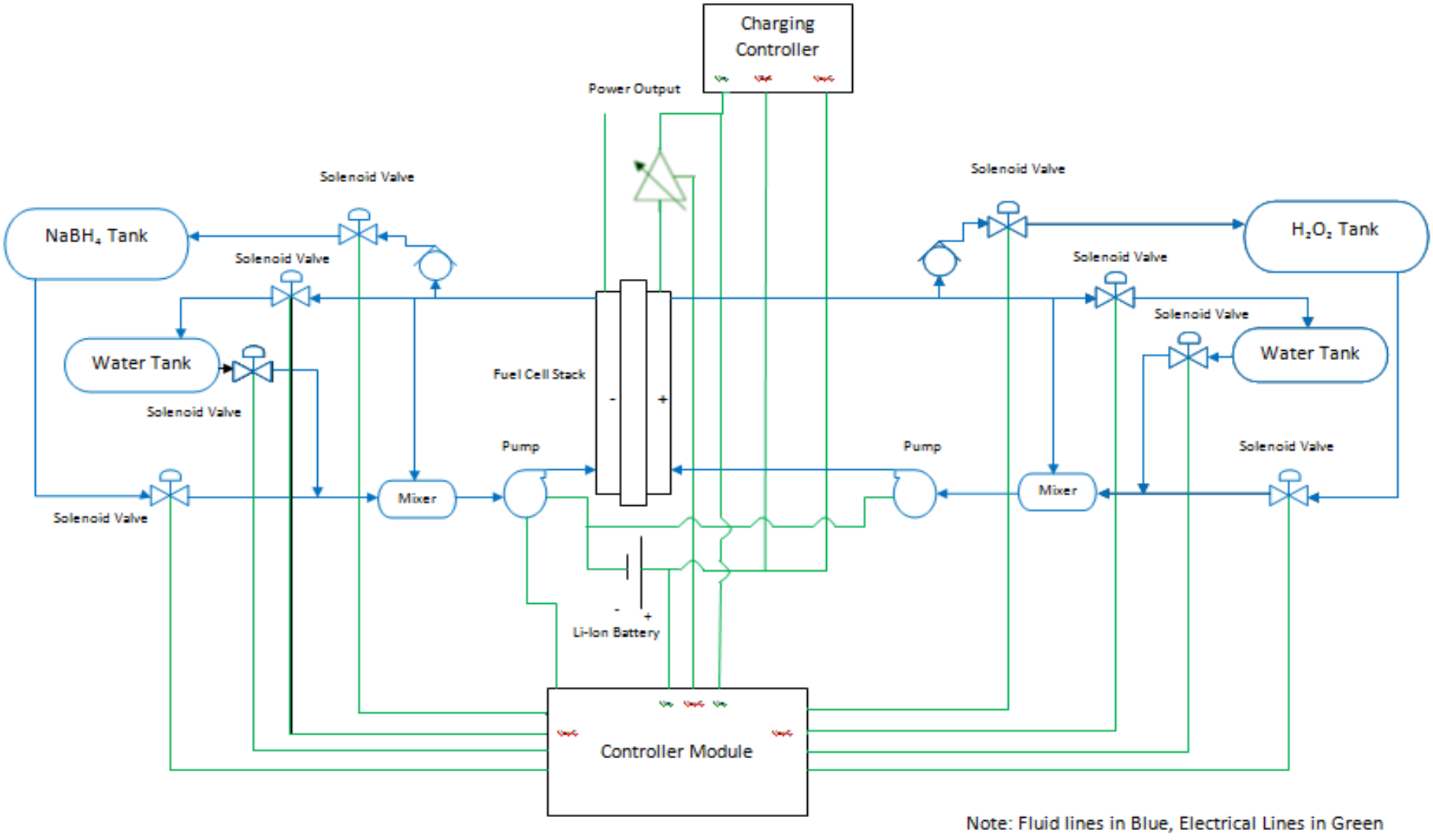

Figure 21: Control System Schematic

The charging controller also regulates incoming voltages via the use of PWM. However, it can only act as a step-down regulator and therefore there is a need for the step-up DC-DC converter. While the system is running, a prescribed load is applied to the fuel cell, further causing the voltage of the fuel cell to decrease. The fuel cell was designed such that a maximum external load of 100 Watts can be applied while still allowing the cell voltage to remain above the 9 V limit of the regulator.

As discussed earlier, the maximum possible power generation capabilities of a fuel cell decrease over time due to gradual reduction in fuel and oxidizer concentration. In order to avoid this, a separate recirculation loop was set up. When the system begins operating, the fuel is first drawn through the tank and re-circulated in the "mixer" loop until the voltage of the cell is too low. At this point, the solenoid valve going back to the tank is then opened such that old fuel is purged and new fuel is injected into the loop. Within the fuel tank, there is another expandable storage bladder which holds the spent fuel. As the quantity of fresh fuel decreases, the amount of spent fuel will linearly increase. This "tank-within-tank" design reduces the need for storage space associated with a second spent fuel tank. The one way valves are installed to ensure there is no back flow of fuel and/or oxidizer when the pumps are turned off.

The water tank is used to clean the fuel cell after each run. This is necessary because the fuel-side byproduct (sodium metaborate) can condense out in the solid phase at room conditions. This can lead to obstruction of channels within the fuel cell and piping. Pumping water through the system also ensures that the sensitive membrane remains hydrated.

The above described operation of the fuel cell ensures that there is always adequate fuel for maximum power production. From equations 3 and 4, it is clear that for every mole of fuel,

four moles of oxidizer are required. Similarly, on a mass basis, the equivalent ratio is $NaBH_4$: $4H_2O_2$. However, for the purposes of this project, a 20% $NaBH_4$ solution and 30% H_2O_2 hydrogen peroxide solution was used. On such a volume basis, however, each liter of fuel solution requires one liter of oxidizer solution.

The fuel solution contains 15% sodium hydroxide (NaOH) and 15% ammonium hydroxide (NH_4OH) with the remainder of the solution being water. The percentages are listed on a mass basis. In the presence of only water, the reaction between water and sodium borohyride is extremely exothermic and causes severe decomposition of the fuel [25]. For stability reasons, a base such as sodium hydroxide is required to prevent this reaction. The Ammonium Hydroxide is required for further stability of the fuel as it undergoes reactions in the fuel cell. The oxidizer solution contains 30% hydrogen peroxide (H_2O_2), 8% sulfuric acid (H_2SO_4) and 5% phosphoric acid (H_3PO_4). Although hydrogen peroxide will not readily dissociate in water under room conditions, it can at elevated temperatures and under the presence of a current. Therefore, the two acids are added for stability of the oxidizer under normal fuel cell operating conditions.

4.3 Actual Control Algorithm

The desired operational characteristics of the control system and fuel cell have been described. However, due to unseen circumstances, the actual operation of the current control system is different. The fuel cell design had to be modified several times over the course of the project as described in earlier sections. Due to the high generation rate of gases, it was not possible to have a completely closed “mixed” recirculation loop due to internal pressure generation. Thus, only one open circulation loop was utilized. Several holes were drilled in the

top of the fuel and oxidizer containers so that any gases could be expelled to the atmosphere. Due to the generation of these gases, it was not possible to have a "tank-within-tank" design for depositing the spent fuel. Because the "mixed" recirculation loop was removed, it no longer made sense to have such a separation of fresh fuel and spent fuel. Besides, the presence of gas in the waste would mean that the inner bladder would expand too quickly compared to the rate of decrease of fresh fuel. Therefore, the proposed design would not work correctly. The use of one-way valves was deemed unnecessary because the gas generation in the fuel cell creates a high pressure and will naturally flow to the low pressure location in the storage tanks even if the pumps are turned off.

Figure 22 shows the system with the fuel cell and all the ancillary equipment. The current operation of the fuel cell begins by a manual switch which opens both solenoid valves leading into and out of the storage tanks. The fuel and oxidizer pumps are turned on at which point, the fuel cell voltage begins rising. At the preset voltage, the controller automatically switches power for the ancillary equipment to begin drawing from the fuel cell instead of the battery. The external load is applied and the fuel cell keeps running until a minimum of 5 V is reached under load. The minimum set point is arbitrary because the DC-DC converter cannot regulate voltages lower than 9V. However, at lower voltages, the pumps and solenoids will still operate. The solenoids will stay open, but the pumps will have a reduced flow rate. At this point, the pumps are stopped and the external load is disconnected. The ball valves leading to the water tanks are immediately opened to allow any release of pressure while the second switch is activated to allow circulation of water. This will remove any residual chemicals and heat while ensuring enough water is supplied to the membranes. Current testing results show that every liter of fuel and oxidizer only allows for thirty minutes of continuous operation before the voltage level is too

low. This, as discussed, is due to the nickel foam which is theorized to cause rapid decomposition of the hydrogen peroxide and to a much lesser extent, the sodium borohydride.

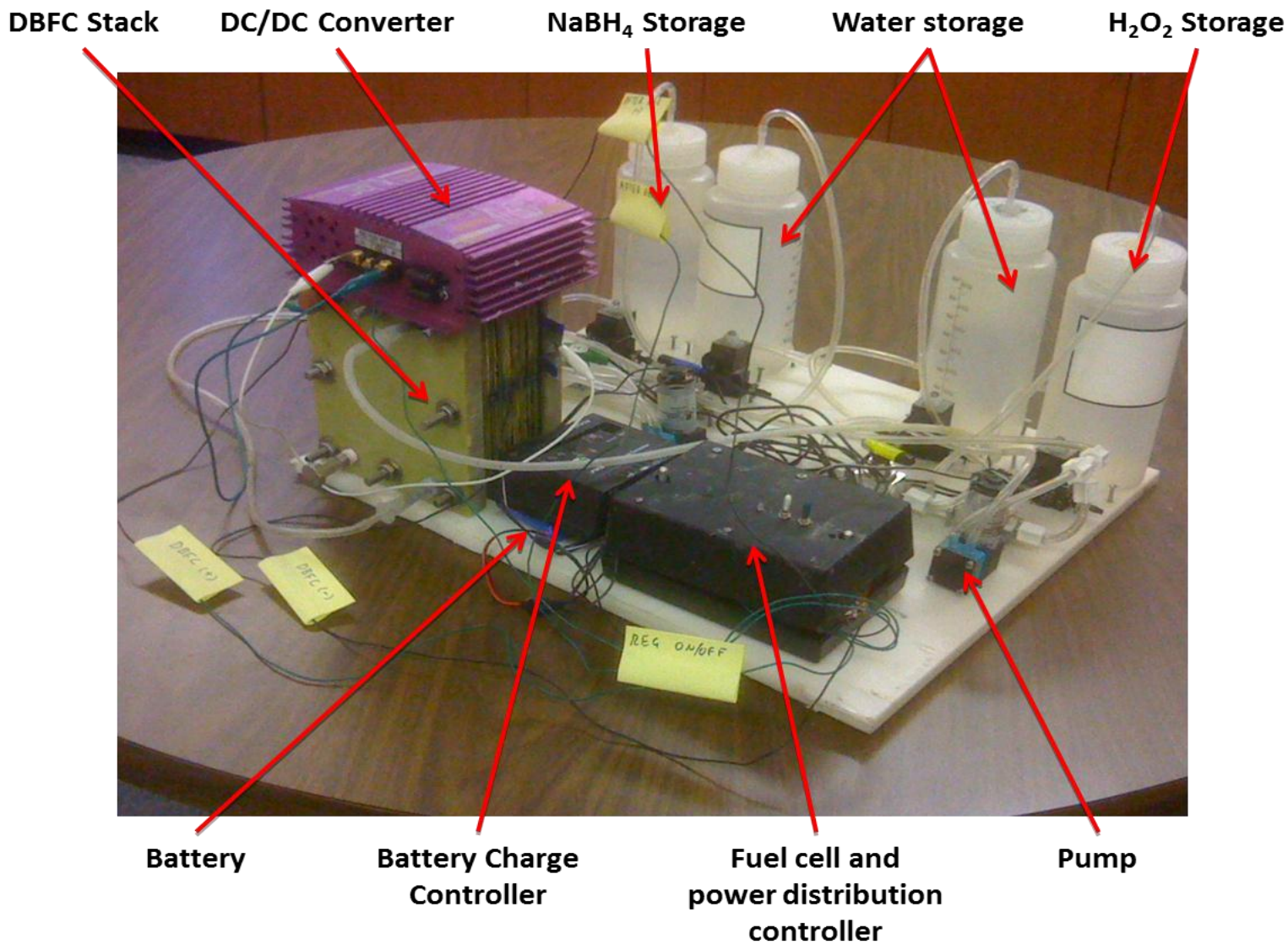

Figure 22: Complete System

4.4 Performance of Second Cell with Control System

The control system was demonstrated with the second fuel cell stack. At 12 volts, the control system will draw approximately 3 amps of current. Therefore, for a normally operating stack, it needs to produce a minimum of 136 watts. The control system was not ready for testing with the first stack, and because the team was not able to replicate its performance, the second stack was used instead.

First, the pumps and solenoids were started using battery power. The fuel cell voltage reached 15 V at which point the control system power was switched to the fuel cell. No external load was applied at this point. The power requirements of the control system dropped the voltage of the stack to 8.7 V. This low voltage is below the 9 V threshold for the DC-DC converter. Therefore, the pumps were now operating at 8.7 V instead of the 12 Volts that the converter could have provided. Thus, the pumping rate was decreased. Nevertheless, it was still enough to keep the fuel and oxidizer moving through the stack. Figure 23 shows the performance of the cell with the control system. The stack achieved 54 W at 4.5 Volts and 12 Amps.

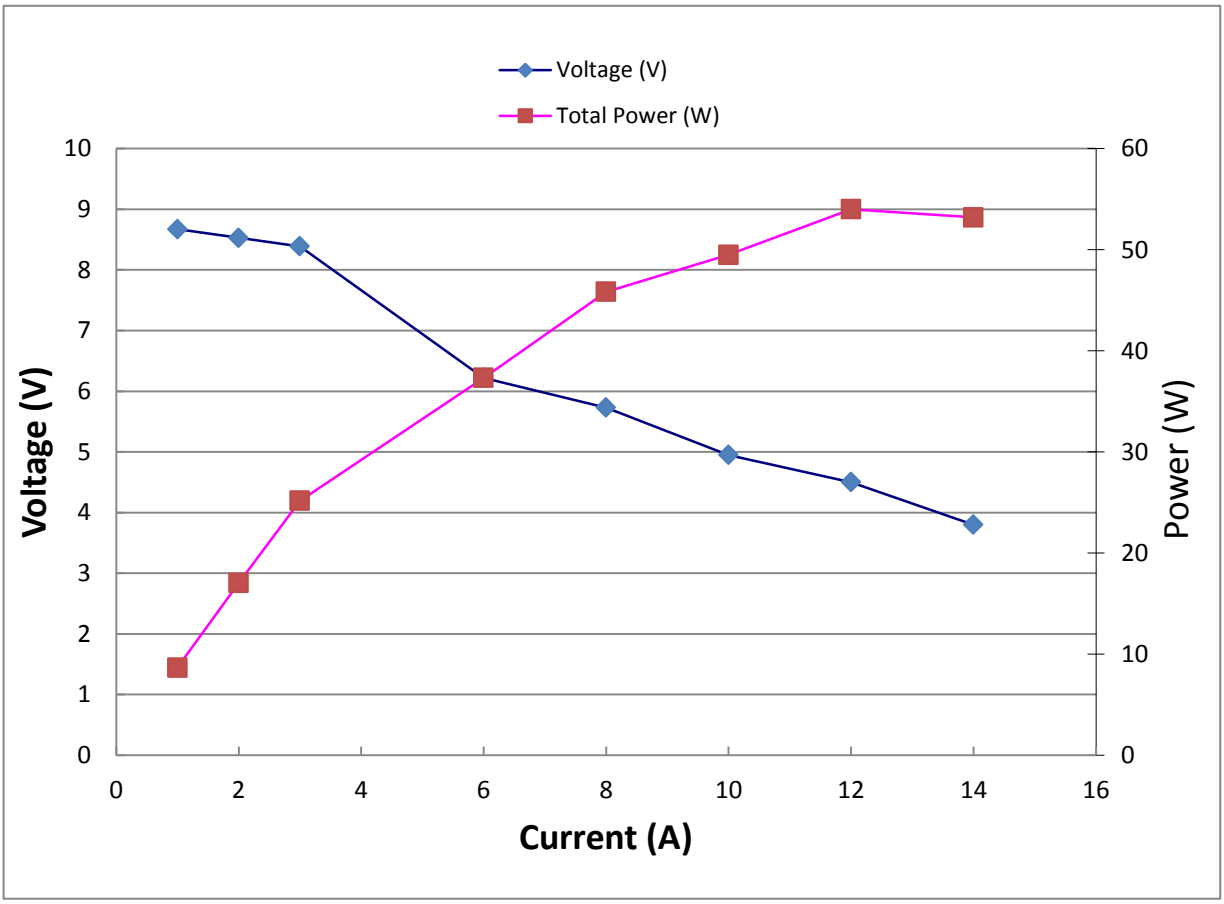

Figure 23: Second Stack Performance with Control System

Thus, with the control system, the fuel cell can still provide 54 W to an external load, or 5.6 W/cell which is a 60% reduction in performance over the original stack. Although the exact power requirements of the controls are not known, they are estimated to consume an additional 10–15 watts. This lower power requirement, as compared with the 36 watts mentioned earlier, is because solenoids and pumps scale down their power draw as a function of voltage. At the peak power of 54 W at 4.5 V, the solenoids remain open but pumping power is drastically reduced. This low flow cannot remove heat and gas adequately. Therefore, the cell cannot be run for too long under these conditions. The same stack showed a maximum power of 50 W without a control system. However, the stack was not heated up during this test and thus did not achieve its maximum performance.

CHAPTER 5: FUTURE DESIGN RECOMMENDATIONS

There are several ways to improve the control system and fuel cell to account for the gas generation and allow for better fuel utilization of the system assuming that the improved fuel cell design does not use nickel foam as a supporting layer. Although there will be some small gas generation due to side reactions, this effect will not be as pronounced.

5.1 Fuel Cell Stack and Liquid Distribution Network

To alleviate problems seen within the stack a proposed solution has been developed and shown in Figure 24. The secured manifold should prevent crossover within the stack. Because both the cover and bipolar frames are thinner, the overall bipolar plate should remain the same thickness.

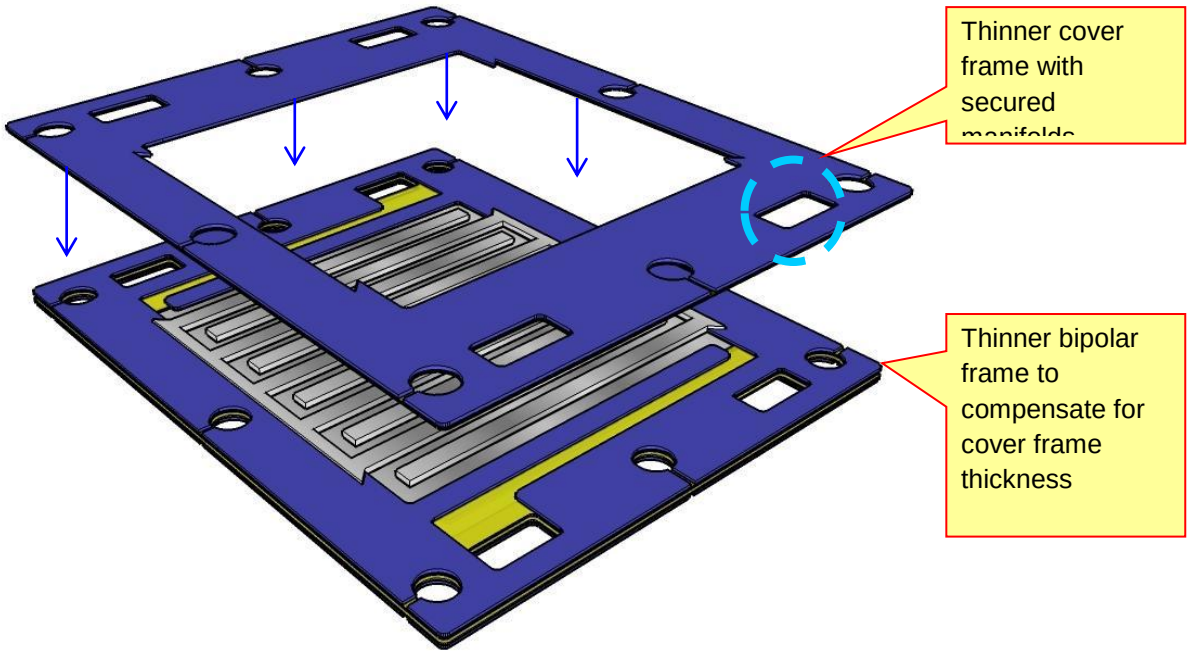

Figure 24: Proposed Bipolar Plate Redesign [21]

Instead of the plugs used on the current cell, hydrophobic vents will be installed. These vents are typically composed from a hydrophobic material such as Teflon and are micro-porous to allow gas to escape. The vents are designed with threads and can be easily incorporated into the fuel cell. Any small amount of gas which is generated should escape the cell via these vents. In this manner, it will be possible to employ a double recirculation loop, as shown in Figure 21, without negatively affecting the cell.

Due to the size of the stack and the control system, the peak power produced by the fuel cell resulted in a voltage drop that was too low for the DC-DC converter. This is primarily due to the capacity of the converter (150 watts). The original intent of this voltage converter was to also regulate the voltage of the external applied load. However, upon further consideration, it was deemed unnecessary to regulate this external load. There are two possible solutions for this issue. The first is to add additional bipolar plates such that the voltage level is high enough at the required power. However, this results in additional mass of the system and inadequate utilization of the stack. Alternatively, the use of a smaller capacity power converter provides a simple and effective solution. The control system and balance of plant only requires approximately thirty watts of power to operate. This level of power is adequate for larger stacks since the pumps used for this setup have a flow rate capacity which is more than twice the required amount. A smaller capacity power converter has the ability to accept a wider range of incoming voltages. This method will allow for greater flexibility in operation of the stack.

The production of gas within the current system resulted in problems after the solenoids were deactivated. When the solenoids are shut, the gas cannot escape and pressure builds up within the system. The weakest point, usually the tubing connection, will burst and potentially release the chemicals and hot gases. To counter this, the connections and fittings should be able

to withstand higher pressures. Ideally, stainless steel should be used because compression fittings made from this material are capable of withstanding pressures greater than 5000 psi. Furthermore, it is also resistant to corrosion which is extremely important when hot corrosive gases and hydrogen peroxide is present. As suggested before, hydrophobic vents should alleviate this problem as well.

One of the most important components that need to be added to the system is a heat exchanger. The nickel foam used in the fuel cell results in exothermic reactions on both the anode and cathode sides. This is favorable for cell reaction kinetics to a certain extent. However, after some time, the increased temperature results in reaction rates which produce more gas and a greater amount of heat. These two effects simultaneously increase the pressure within the system. The high temperature can be detrimental to components of the cell. Because each bipolar plate is thermally conductive, the fuel and oxidizer both experience similar temperature increases. Therefore, a heat exchanger should be able to cool both the anode and cathode. Careful consideration is required in the design of such a heat exchanger. The temperature needs to be kept high enough such that sodium metaborate does not condense and remains soluble within the fuel solution.

5.2 Control System

When used in UAV applications, there may be a need for instantaneous peak power. This could occur due to the need of sudden acceleration or the use of some other component. Because fuel cells cannot generally handle fast transient loads due to their slow internal electrochemical and thermodynamic responses [26], a hybrid architecture become necessary. The control system proposed here needs to be modified to be capable of handling these transient loads. Depending

on the system's needs, a battery and/or super capacitors can be considered. Using appropriate methods, the control system should use the fuel cell for base load energy generation with the battery and/or super capacitors being used for transient and peak loads. The system should be analyzed for dynamic load response, mass, and volume. Various fuel cell hybrid systems have been previously studied for UAV applications [27–28] and can provide deeper insight for future design considerations.

To successfully integrate the control system into a hybrid architecture, the capability to measure current is necessary. During operation of the current system, it was not possible to accurately determine the power needed. This could easily be achieved through an induction type current measurement sensor. These types of sensors are commercially available, and can be easily implemented into the current system using a variable voltage output.

CHAPTER 6: CONCLUSIONS

In summary, the team was able to develop a novel and unique integrated manifold direct borohydride fuel cell stack and control system capable of providing 100 Watts at 140 mW/cm^2. The first stack was able to provide adequate power. However, due to internal mixing, deterioration within the stack resulted in decreased performance. Due to funding limitations, a "quick" patch correction was tried in a revised second cell. The fix, however, required a thick filler layer which ultimately decreased cell performance by 60%. Nevertheless, the successful operation of this stack with the control system was demonstrated. A redesign has been identified that should remove the problems seen in the second stack and achieve the power levels seen in the original stack.

REFERENCES

[1] J. Larminie, A. Dicks, *Fuel Cell Systems Explained*, Wiley, 2004.

[2] Valdez, T. I. et al. "Sodium Borohydride/Hydrogen Peroxide Fuel Cells for Space Application." 209th Electrochemical Society Meeting. California, Los Angeles. 12 Feb. 2011. Lecture.

[3] C. Ponce de Leon, F.C. Walsh , D. Pletcher, D.J. Browning , J.B. Lakeman, *Journal of Power Sources* 155 (2006) 172–181.

[4] R. P. O'Hayre, S. Cha, *Fuel cell fundamentals*, Wiley, 2005.

[5] R. X. Feng, H. Dong, Y.D. Wang, X.P. Ai, Y.L. Cao, H.X. Yang, *Electrochemistry Communications.* 7 (2005) 449.

[6] B.H. Liu, Z.P. Li, S. Suda, *Electrochimica. Acta.* 49 (2004) 3097.

[7] S.C. Amendola, P. Onnerud, M.T. Kelly, P.J. Petillo, S.L. Sharp-Goldman, M. Binder, *Journal of Power* Sources 84 (1999) 130.

[8] R.K. Raman, A.K. Shukla, *Journal of Applied Electrchemistry*. 35 (2005) 1157.

[9] N. Choudhury, R.K. Raman, S. Sampath, A.K. Shukla, *Journal of Power Sources*. 143 (2005) 1.

[10] R.K. Raman, N.A. Choudhury, A.K. Shukla, *Electrochemical and Solid State Letters* 7 (2004) A488.

[11] R.K. Raman, S.K. Prashant, A.K. Shukla, *Journal of Power Sources* 162 (2006) 1073.

[12] W. Jaijun, W. Cheng, L Zhixiang, M. Zongqiang, *International Journal of Hydrogen Energy*. 35 (2010) 2648.

[13] L.Gu , N. Luo, G.H. Miley. *Journal of Power Sources* 172 (2007) 77–85.

[14] *Hydrogen Fuel Cell Engines and Related Technologies*. DOE Energy Efficiency and Reneweable Energy Office. Dec. 2001.

[15] J. Das et al. *Chemical Communications*. 42 (2009) 6394-96.

[16] L. Gu, N. Luo, G.H. Miley, *Journal of Power Sources* 173 (2007) 77.

[17] K. Wonslyd, E. Christensen, Q. Li, J.O. Jensen, "High Temperature Polymer Electrolyte Membrane Water Electrolysis Cells". <http://materialsknowledge.org/docs/Poster-Karen_Wonsyld.pdf>.

[18] A. Heinzel, F. Mahlendorf, C. Jensen, "Bipolar Plates". 2009. Elsevier.

[19] E. Carlson, N. Garland, R. Sutton, "Cost Analyses of Fuel Cell Stack/Systems". *Hydrogen, Fuel Cells, and Infrastructure Technologies.* Report, 2003.

[20] *Bipolar Plates.* Photograph. *Ajusa*. Web. 16 Mar 2012. <www.ajusa.es/eng/imasdemasi/componentes.html>.

[21] Image courtesy of Dr. Kyu-Jung Kim, Research Assistant Professor, University of Illinois at Urbana-Champaign.

[22] M. Simoes, S. Baranton, C. Coutanceau, C. Lamy, J. Leger, *ECS Transactions* 25 (2009) 1413.

[23] H. Yang, T.S. Zhao. *Electrochimica Acta* 50 (2005) 3243–52.

[24] *Nickel (III) Sulphate*. Photograph. *Science Photo Library*. Web. 16 Mar. 2012. <http://www.sciencephoto.com/media/4447/enlarge>.

[25] F.A. Cotton, G. Wilkinson, *Advanced Inorganic Chemistry***,** 5th ed. Wiley & Sons, New York (1988).

[26] C. Wang, M. H. Nehrir, and S. R. Shaw, *IEEE Transactions on Energy Conversion*, 20 (2005) 442–451.

[27] Q. Cai, D.J. Brett, N.P. Brandon, "Hybrid Fuel Cell/Battery Power Systems for Underwater Vehicles", *3rd SEAS DTC Technical Conference*, Edinburgh 2007.

[28] V. Yufit, N.P. Brandon, *Journal of Power Sources 196* (2011) 801-807.